06,13

Preparation, structural features, elemental composition of and dielectric properties of a two-layer structure based on thin films of multiferroic $BiFeO_3$ and ferroelectric $(Sr, Ba)Nb_2O_6$

© A.V. Pavlenko[1,2], D.V. Stryukov[1], Yu.A. Kudryavtsev[3], Ya.Yu. Matyash[1], N.V. Malomyzheva[2]

[1] Southern Scientific Center, Russian Academy of Sciences, Rostov-on-Don, Russia
[2] Scientific Research Institute of Physics, Southern Federal University, Rostov-on-Don, Russia
[3] Solid State Electronics Section, Cinvestav-IPN, Mexico

E-mail: Antvpr@mail.ru

Received July 14, 2022
Revised July 14, 2022
Accepted July 18, 2022

BiFeO heterostructures were manufactured using intermittent sputtering technology on the surface of a single crystal substrate MgO(001) $BiFeO_3/(Sr, Ba)Nb_2O_6$. Studies of the structure, thickness profile of the composition, surface morphology and dielectric characteristics of materials have been carried out. It is established that despite the formation of two types of orientation domains ($\pm 18.4^\circ$) in the layer $(Sr, Ba)Nb_2O_6$, the upper layer of $BiFeO_3$ is in the ratio of the total parallel orientation with the substrate MgO(001). It is shown that the composition of the films of bismuth ferrite and barium-strontium niobate does not change in film thickness, corresponds to the compositions of the sprayed ceramic targets, no signs of the presence of buffer layers were revealed. The results of the study of dielectric and ferroelectric characteristics of the heterostructure are presented. The reasons for the revealed patterns are discussed.

Keywords: thin films, heterostructure, barium-strontium niobate, bismuth ferrite.

DOI: 10.21883/PSS.2022.12.54387.439

1. Introduction

Currently, ferroelectric and multiferroid directions in physical materials science are at the stage of rapid development, due to the use of these active materials in microelectronics, telecommunications systems, sensors and sensors [1]. Depending on the operating conditions and purpose, they can be used in the form of ceramics (power devices), single crystals (holography) or thin films (memory elements, MEMS). If in the case of ceramics and single crystals, the way to control properties is to change their composition [2], then additional control possibilities open up for composites and heterostructures based on thin films, for example, by using the effects of deformation and domain engineering [3], creating *n*-layered structures in which materials with known parameters act as a layer. The resulting properties of *n*-layered structures can be either superpositions of the properties of each of the layers, or they can be fundamentally new, depending on the order and thickness of the layers [4]. In the manufacture of multilayer layers, the same type of structures are most often used, or rather close ones, since in this case the technological complexity of the growth of layers of high structural quality is minimized. This is well demonstrated for materials with a perovskite-type structure ($BiFeO_3$, $BaTiO_3$, PZT, etc.) [1,5,6]. A promising set of properties, from our point of view, can be realized in heterostructures based on materials with the structure of perovskite and tetragonal tungsten bronzes, in particular – bismuth ferrite ($BiFeO_3$ (BFO) — multiferroic with $T_C = 1083\,\mathrm{K}, T_N = 643\,\mathrm{K}$, $P \sim 100\,\mu\mathrm{C/cm^2}$) and barium-strontium niobate ($(Ba, Sr)Nb_2O_6$ (SBN) — uniaxial ferroelectric, successfully used depending on the composition in pyropriemniki, nonlinear optics and optical modulators [7]). The possibility of obtaining heteroepitaxial BFO and SBN films under sufficiently similar technological conditions using a single-stage RF cathode sputtering method is shown in [8,9]. In this paper, we present the results of studies of the phase composition, distribution profile of structure-forming elements, crystal structure and dielectric properties of the BFO/SBN/MgO(001) heterostructure.

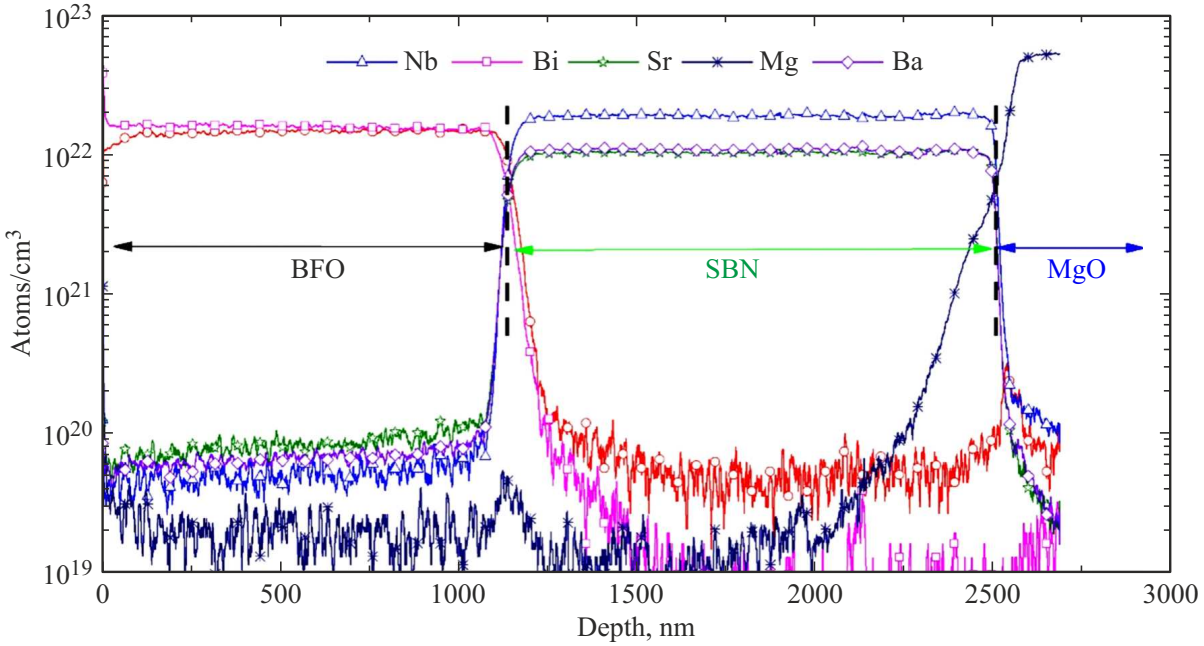

Figure 1. The thickness distribution profile of Bi, Fe, Ba, Sr, Nb, O, Mg atoms in the BFO/SBN/Mg(001) heterostructure.

2. Research targets. Methods of obtaining and research

A single crystal plate of MgO cut (001) 0.5mm thick was used as a substrate. The films were sprayed by high-frequency spraying in an oxygen atmosphere at the „Plasma 50–SE" installation using technological modes [8,9]. X-ray diffraction studies were carried out on a multifunctional X-ray complex „RIKOR" (goniometer with increments up to 0.001° (Crystal Logic Inc.); X-ray tube BSV21-Cu (JSC „Svetlana-Roentgen"), scintillation detector (LLC ITC „Radikon"). The morphology of the surface was studied on an atomic force microscope „Ntegra Academia" company NT-MDT (Russia) at a temperature of 23°C. Scanning was carried out in semi-contact mode using a silicon cantilever NS15/50 (equipment of the Joint Center for Scientific and Technological Equipment of the UNC RAS (research, development, testing) (№ 501994)).

The profiles of the distribution of atoms over the thickness of the heterostructure were measured by secondary ion mass spectrometry using a time-of-flight mass spectrometer TOF-SIMS-V of Ion-TOF GmbH. Profiling was carried out in the „mode of a double beam": spraying of the surface on an area of $300 \times 300\,\mu$m was carried out by a beam of Cs+ ions with an energy of 0.5 keV; secondary positive cluster ions CsM+ were analyzed (where M — the element of interest), sprayed from the central part ($100 \times 100\,\mu$m) of the etching crater by a pulsed ion beam Vi^{3+} with an ion energy of 30 keV. The angle of incidence for both ion beams was 45°. The depth of the experimental crater was measured by a Bruker profilometer DektakXT; the data obtained were used to recalculate the etching time to depth in the experimental profile. A low-energy electron source (20 keV) with a beam current of $17\,\mu$A was used to compensate for the surface charge during profiling.

Measurement of the relative permittivity ($\varepsilon/\varepsilon_0$) and the tangent of the dielectric loss angle ($\mathrm{tg}\,\delta$) in the frequency range of the measuring eclectic field $f = 20-10^6$ Hz with an amplitude of 40 mV was obtained with using a measuring stand based on LCR meter Agilent 4980A. Measurements of $P(U)$ characteristics at $T = 24$°C were carried out on the TFAnalyzer2000 analyzer. Temperature control during measurements was carried out by the Linkam THMS600 stage system.

3. Experimental results and discussion

Figure 1 shows the distribution profile of Bi, Sr, Ba, Fe, Nb and Mg atoms over the thickness of the manufactured sample, which are structure-forming for bismuth ferrite, barium-strontium niobates and magnesium oxide, respectively. The analysis of the results showed that the composition of each of the deposited layers does not change in the thickness of the BFO/SBN/Mg(001) heterostructure and corresponds to the composition of the sprayed ceramic targets — $BiFeO_3$ and $(Sr_{0.50}Ba_{0.50})Nb_2O_6$. As we have shown in [8,10], heteroepitaxial single crystal SBN films are characterized by a developed surface morphology, since within the framework of the technology used, their growth occurs by the Vollmer–Weber mechanism (Fig. 2). However, despite the small value of the RMS roughness

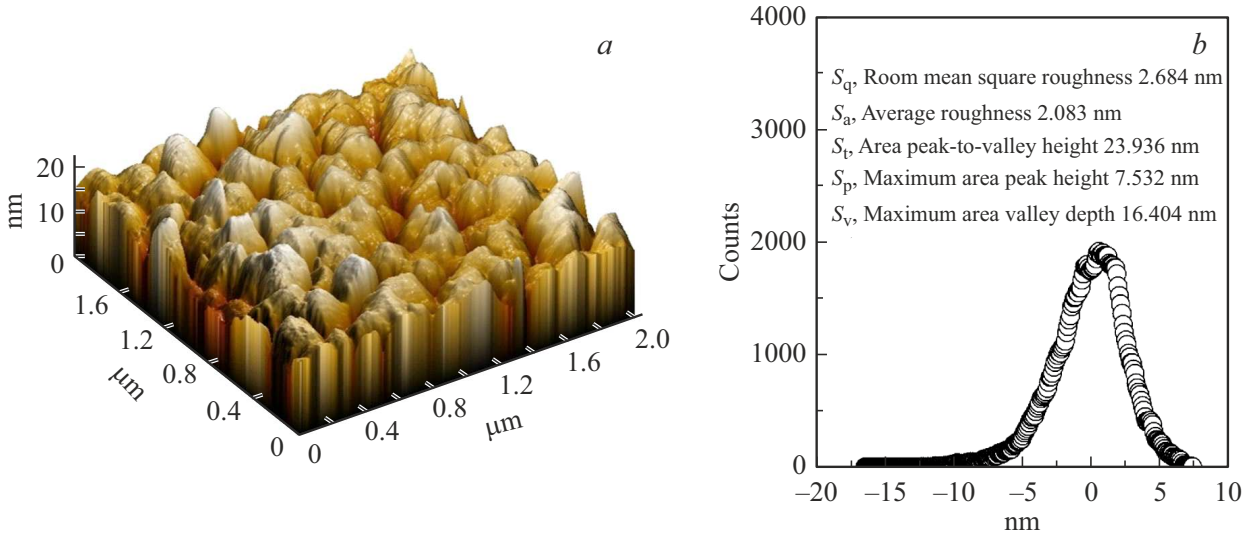

Figure 2. AFM surface images and height distribution histogram for SBN/MgO film.

of the SBN film surface ($S_q = 2.68$ nm), the height difference on a typical film surface area of $4\,\mu m^2$ reaches $S_R = 23.936$ nm. Such roughness affects the experimental profile of the interface of the layers: the experimental profile of the VIMS, as is known [11], is an integral convolution of the real distribution of elements and surface roughness. There are no signs of doping of the SBN film with chemical elements from the bismuth ferrite layer deposited by the latter, as well as the presence of transition layers at the interface of BFO → SBN and SBN → MgO is not fixed. The results of X-ray diffraction analysis presented below also testified in favor of this. All the obtained radiographs of the BFO/SBN/MgO(001) heterostructure showed only reflections from the layers of the heterostructure and the substrate, which confirms the absence of impurity phases (Fig. 3, *a*). This is consistent with the fact that the radiograph of BFO ceramics (Fig. 3, *a*), which was the target during spraying, also does not contain visible traces of impurities. On the survey $\theta - 2\theta$ radiograph, only reflections from the planes of the family (*00l*) of both layers of the heterostructure were present, and on φ-scans (Fig. 3, *b*) — clear maxima for each of the layers, which proves the epitaxial growth of the heterostructure layers. SBN was obtained with the formation of orientation domains deployed in the interface plane at $\pm 18.4°$ relative to the axes of the substrate, and BFO was obtained with the orientation of the crystallographic axes parallel to the axes of the substrate. When analyzing the swing curves, it was found that for BFO they are double, but when rotated by φ by 45° they become single (Fig. 4). An additional 45° turn by φ again makes the swing curve double again. The distance between the two maxima is 0.7°. From our point of view, such bifurcation of reflections on swing curves is due to the tilt of the axis [001] by 0.35°, as in BFO/MgO(001) [9]. Even in the case of double lines, the half-width of the swing curve does not exceed 1.5°, which indicates a high structural perfection of the heterostructure and a low misorientation of the crystallographic axes in the direction of the normal to the substrate plane.

The parameters of the elementary cells of each layer of the BFO/SBN/MgO(001) heterostructure in the direction of the normal to the substrate surface were $c_{SBN} = 3.960(1)$ Å, $c_{BFO} = 3.970(1)$ Å. To determine the parameters of the unit cell in the interface plane, $\theta - 2\theta$ X-ray images of reflexes (113) were obtained BFO layer and (313) of the SBN layer in an asymmetric geometry (Fig. 5). More intense reflexes (103) The parameters of the BFO layer were not taken into account, since it is not possible to reliably separate them from the reflexes (313) of the SBN layer. For each angle φ, two reflexes (113) of the BFO layer were observed (Fig. 5, *a*) with different rotation angles in the asymmetric geometry used. Their positions correspond to an elementary cell with an axis slope of c by 0.35°. Since a similar situation is observed when φ is rotated by 90°, therefore, in the BFO layer there are crystallites with four elementary cells with the same parameters $a = b = c = 3.970$ Å, but different angles: 1) $\alpha = \gamma = 90°$, $\beta = 89.65°$; 2) $\alpha = \gamma = 90°$, $\beta = 90.35°$; 3) $\alpha = 89.65°$, $\beta = \gamma = 90°$; 4) $\alpha = 90.35°$, $\beta = \gamma = 90°$. The parameters of the lattice of BFO ceramics, which was the target during spraying, are: $a = 3.9618$ Å, $\alpha = 89.45°$. Comparing the obtained parameters of the film lattice with the parameters of ceramics, it can be seen that there is a slight tensile strain of 0.2SBN layer, for each of the orientation domains there are eight reflexes (313), four of which are observed without overlapping other reflexes. These reflexes were used to calculate the

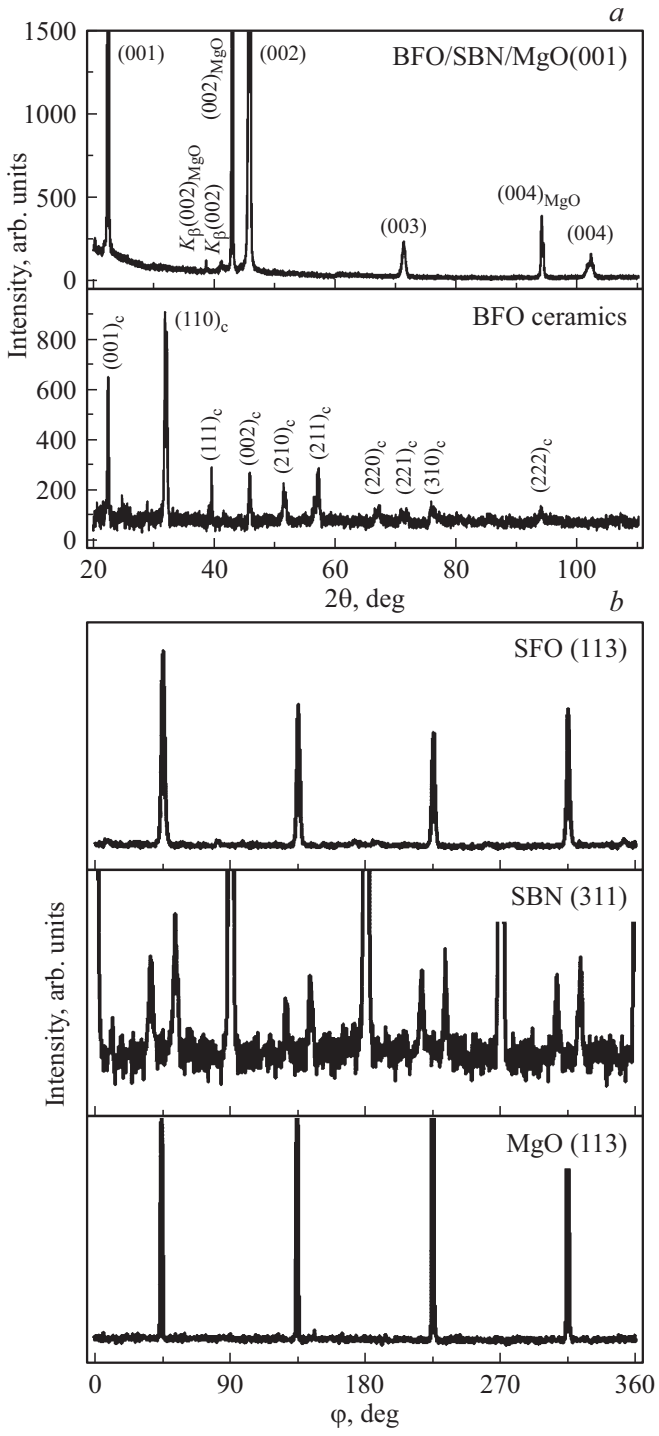

Figure 3. Overview $\theta - 2\theta$-radiograph of the BFO/SBN/MgO heterostructure(001) (*a*); φ — x-ray images of reflexes (113) BFO layer, (221) SBN layer and (113) MgO substrates (*b*).

parameter a in the interface plane. The reflex (313) for two orientation domains has the same angular position, and a φ rotation by 90° does not lead to a shift in the positions of the maxima (Fig. 5, *b*), which indicates the equality of the parameters $a = b$ for them. Thus, the SBN layer, as in the case of single-layer structures, has a tetragonal unit cell with the parameters: $c = 3.960(1)$ Å; $a = b = 12.59(1)$ Å.

To analyze the dielectric properties of the material in the direction perpendicular to the surface, capacitor structures Ag/BFO/SBN/Pt(001)/MgO(001) were manufactured. When $T = 24°$ with the value of the effective $\varepsilon/\varepsilon_0$ two-layer structure varies from 230 (at $f = 2$ MHz) to 445 (at $f = 120$ Hz), and $\operatorname{tg}\delta$ with increasing frequency gradually decreases from 0.18 to 0.05 (fig. 6). This indicates the presence of dielectric dispersion in the material. When measured in weak electric fields, the sample under study, taking into account the differences in the characteristics of SBN and BFO, should be considered as a two-layer Maxwell-Wagner capacitor [12] with the following dispersion of the complex permittivity [13]:

$$\varepsilon^* = \varepsilon_\infty + \frac{\varepsilon_s - \varepsilon_\infty}{1 + i\omega\tau} - i\,\frac{\gamma}{\omega\varepsilon_0};$$

$$\tau = \varepsilon_0\,\frac{\theta_1\varepsilon_2 + \theta_2\varepsilon_1}{\theta_1\gamma_2 + \theta_2\gamma_1};$$

$$\varepsilon_\infty = \frac{\varepsilon_1\varepsilon_2}{\theta_1\varepsilon_2 + \theta_2\varepsilon_1};$$

$$\varepsilon_s = \frac{\varepsilon_1\gamma_2 + \varepsilon_2\gamma_1 - \tau\gamma_1\gamma_2}{\theta_1\gamma_2 + \theta_2\gamma_1}; \qquad (1)$$

where ε_s — static permeability, ε_∞ — high-frequency permeability, γ — electrical conductivity and τ — relaxation time of the two-layer dielectric as a whole, ε_1, γ_1, θ_1, ε_2, γ_2, θ_2 — dielectric permittivity, electrical conductivity and volume concentrations of the first and second layers, respectively.

Having considered taking into account [14,15] to estimate the value $\varepsilon_1 = 1000$, $\gamma_1 = 10^{-10}\,(\Omega\cdot\mathrm{m})^{-1}$, $\theta_1 = 0.5$ and $\varepsilon_2 = 150$, $\gamma_2 = 10^{-10}\,(\Omega\cdot\mathrm{m})^{-1}$, $\theta_2 = 0.5$ (layer 1 — SBN, layer 2 —BFO) it can be shown that $\varepsilon_s = 575$, $\varepsilon_\infty = 260$ $f_R = 1/\tau = 0.019$ Hz, i.e. in the frequency range $20-10^6$ Hz we make measurements at $f > f_R$ and fix the values of ε_∞, which are close experimentally observed. The value of f_R is important to take into account when analyzing field effects on a sample. Since the dispersion of dielectric characteristics in the corresponding single-layer structures occurs only in the case of SBN, it can be argued that the revealed dispersion $\varepsilon/\varepsilon_0(f)$ is mainly associated with changes in the barium-strontium niobate film. Preliminary work has shown that varying the thickness of the layers allows both increasing and decreasing the value of $\varepsilon/\varepsilon_0$ of the two-layer, while maintaining the values of $\operatorname{tg}\delta$ at the same level.

The ferroelectric properties of the object were clearly manifested when measuring the dependencies of $P(U)$. If in sufficiently small fields the loops had an elongated almost symmetrical shape, then as the amplitude increased, the dependence of $P(U)$ expanded and became asymmetric, the background of the field effect acquired an important role, which complicated their analysis. This

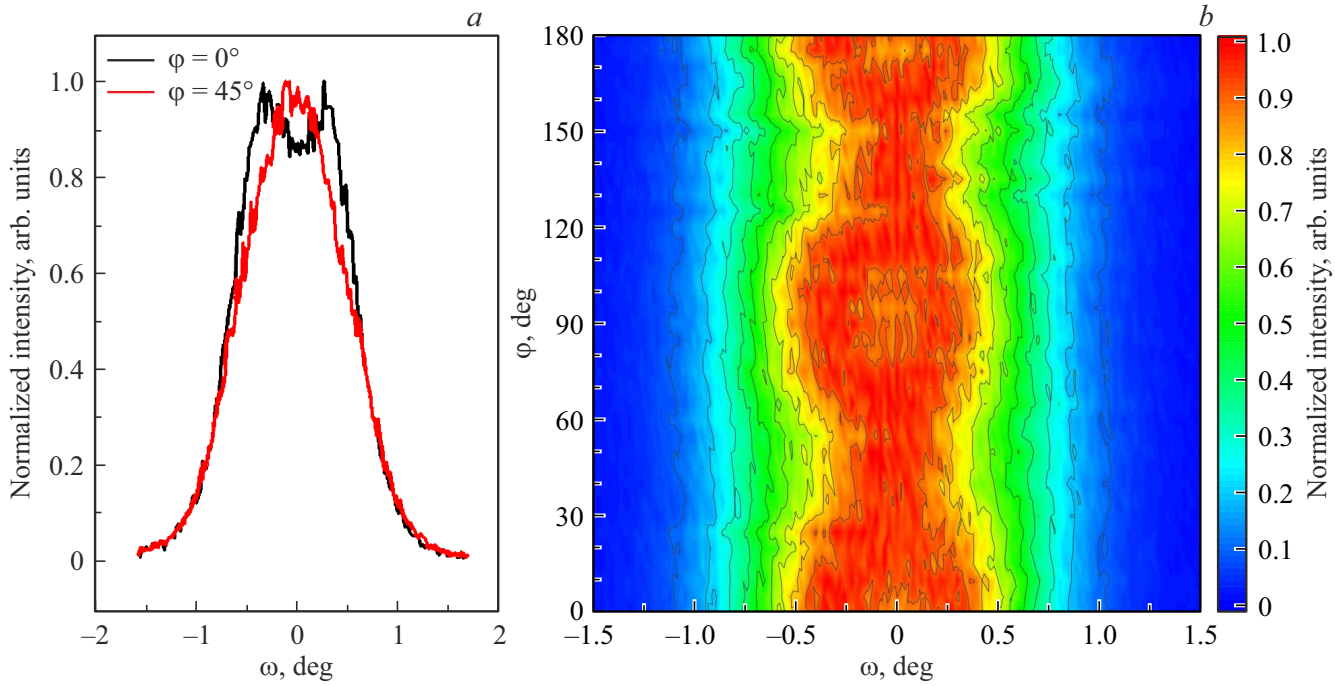

Figure 4. Swing curves (a) and a two-dimensional map of swing curves (b) of the reflex (001) of the BFO/SBN/Mo(001) heterostructure with angle rotation φ.

is due to the difference between the values of the coercive field, spontaneous polarization and dielectric parameters of the SBN and BFO layers. We will carry out more detailed research in this direction in the future. As an example, Figure 7 shows one of these dependencies. When applying a triangular-shaped electric field with an amplitude of 40 V to a two-layer heterostructure of BFO(500 nm)/SBN(500 nm), it was not possible to achieve complete saturation of the loops, while the

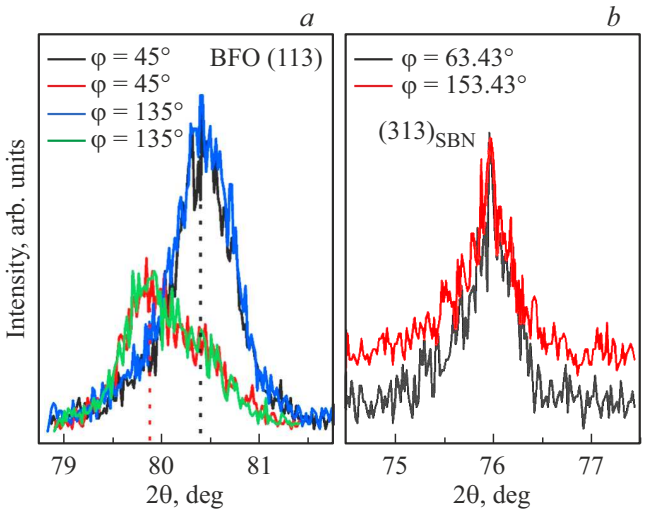

Figure 5. $\theta-2\theta$-X-ray images of reflexes (113) of the BFO layer (a) and (313) of the SBN layer (b) obtained in the asymmetric geometry of the survey.

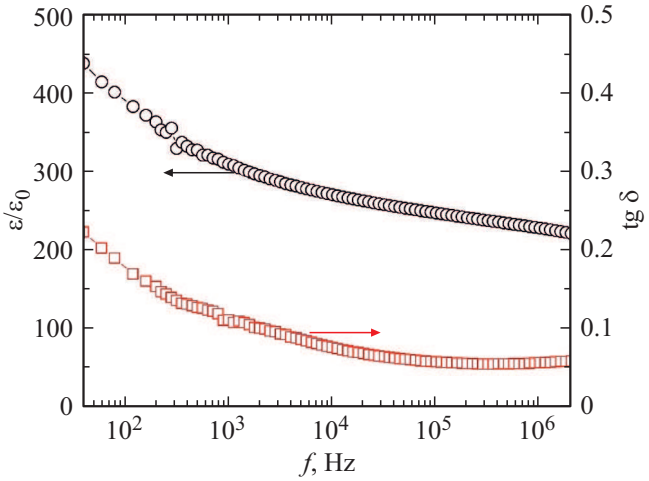

Figure 6. Dependencies $\varepsilon/\varepsilon_0(f)$ and $\mathrm{tg}\,\delta(f)$ heterostructures Ag/BFO/SBN/Pt(001)/MgO(001) at $T = 24°C$.

polarization value at maximum U reached 35 μC/cm^2, and the residual polarization after one cycle of exposure — 7.3 μC/cm^2.

4. Conclusions

1. Using intermittent sputtering technology, BFO/SBN/MgO(001) heterostructures were manufactured in which, according to X-ray diffraction data, impurity phases were absent.

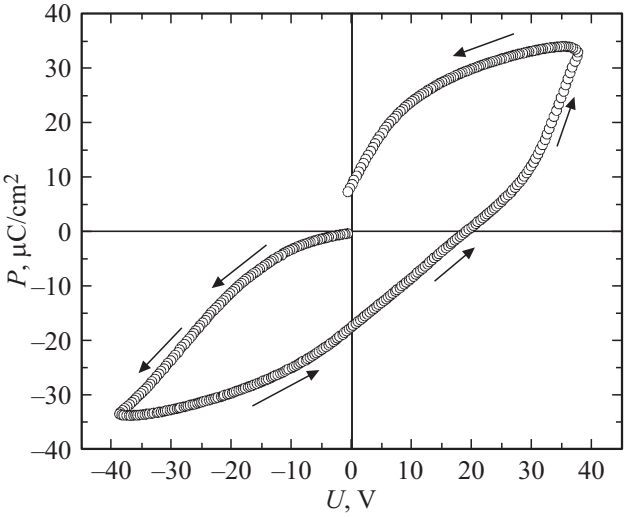

Figure 7. Dependencies of $P(U)$ heterostructures Ag/BFO/SBN/Pt(001)/MgO(001) at $T = 24°C$, $f = 10^3$ Hz, the shape of the acting signal — triangle.

2. It was found that, despite the presence of two types of orientation domains in the SBN layer, the BFO layer grew without rotations of the crystallographic axes relative to the axes of the substrate. This indicates from our point of view that the formation of orientation domains in barium-strontium niobates with a rotation by $\pm 18.4°$ is a natural way of joining both the TVB structure with cubic and related elementary cells, and vice versa.

3. Analysis of the distribution profile of structure-forming atoms using the VIMS method confirmed the preservation of the composition of the layers by the thickness of the deposited films. Mutual diffusion of elements between films and from the substrate to the film is not observed. The increase in magnesium intensity at the SBN-MgO interface is caused by the matrix effect and, in part, by the roughness of the crystal surface MgO.

4. In the study of Ag/BFO/SBN/Pt(001) capacitor structures, it was shown that at room temperature in the range of $f = 20-10^6$ Hz two-layer structure BFO(500 nm)/SBN(500 nm) is characterized by $\varepsilon/\varepsilon_0 = 230-445$ and $\mathrm{tg}\,\delta = 0.05-0.18$, and the value of $P_{\max}$ at $U = 40$ V is 35 uC/cm^2.

5. The obtained results should be used in the study and use of functional materials based on thin films of bismuth ferrite multiferroic and barium-strontium niobate ferroelectric.

Funding

The work was carried out as part of the President's grant MD-483.2022.1.2 and with the support of the scientific project No. G30110/22-01-EP within the framework of the state assignment of the Ministry of Science and Higher Education of the Russian Federation.

Conflict of interest

The authors declare that they have no conflict of interest.

References

[1] Ferroelectric physics. Modern View / Ed . K.M. Rabe, C.G. An, J.-M. Triscon. Translated from English BINOM. Laboratoriya znanij, M. (2011). 440 p. (in Russian).
[2] I.A. Verbenko, E.B. Glazunova, C.I. Dudkina, L.A. Reznichenko. Ekologicheski chistyie intellektualnyie materialy s osobymi elektricheskimi i magnitnymi svoistvami. Puti poiska: modifitsirovanie. Foundation of Science and Education, Rostov-on-Don. (2020). T. 1. 328 p. (in Russian).
[3] A.A. Bukharaev, A.K. Zvezdin, A.P. Pyatakov, Yu.K. Fetisov. UFN, **188**, *12*, 1288 (2018) (in Russian).
[4] D.V. Strukov, V.M. Mukhortov, Yu.I. Golovko, S.V. Biryukov. FTT **60**, *1*, 113 (2018).
[5] B. He, Z. Wang. ACS Appl. Mater. Interfaces **8**, 6736 (2016).
[6] D.P. Pavlov, I.I. Piyanzina, V.M. Mukhortov, A.M. Balashov, D.A. Tayursky, I.A. Garifullin, R.F. Mamin. Pis'ma v ZhETF **106**, *7*, 440 (2017). (in Russian).
[7] S. Gupta, S. Sharma, T. Ahmad, A.S. Kaushik, P.K. Jha, V. Gupta, M. Tomar. Mater. Chem. Phys. **262**, 124300 (2021).
[8] A.V. Pavlenko, D.V. Stryukov, L.I. Ivleva, A.P. Kovtun, K.M. Zhidel', P.A. Lykov. FTT **63**, *2*, 776 (2021). (in Russian).
[9] A.V. Pavlenko, D.V. Stryukov, S.P. Kubrin. FTT **64**, *2*, 218 (2022). (in Russian).
[10] A.V.Pavlenko, S.P.Zinchenko, D.V. Stryukov, A.G. Fedorenko, A. Nazarenko. Neorgan. materialy **57**, *4*, 398 (2021). (in Russian).
[11] Yu. Kudryavtsev, S. Gayardo, A. Viegas, G. Ramirez, R. Azomosa. Izv. RAN. Ser. fiz. **72**, *7*, 949 (2008). (in Russian).
[12] A.R. Hippel. Dielektriki i volny. Translated from English / Ed. N.T. Drozdova. IL, M. (1960). 438 p. (in Russian).
[13] A.S. Bogatin, A.V. Turik. Relaxation polarization processes in dielectrics with high through conductivity. Fenix, Rostov n/D (2013). 256 p. (in Russian).
[14] A.V. Pavlenko, I.N. Zakharchenko, A.S. Anokhin, Yu.A. Kuprina, L.And Kiseleva, Yu.I. Yuzyuk. FTT **59**, *5*, 88 (2017). (in Russian).
[15] R. Yinjuan, Z. Xiaohong, Z. Caiyun, Z. Jiliang, Z. Jianguo, X. Dingquan. Ceram.Int. **40**, *1*, 2489 (2014).